

A distributed control strategy for optimal reactive power flow with power constraints

Saverio Bolognani, Ruggero Carli, Guido Cavraro, and Sandro Zampieri

Abstract—We consider the problem of exploiting the microgenerators dispersed in the power distribution network in order to provide distributed reactive power compensation for power losses minimization and voltage support. The proposed strategy requires that all the intelligent agents, located at the microgenerator buses, measure their voltage and share these data with the other agents on a cyber layer. The agents then actuate the physical layer by adjusting the amount of reactive power injected into the grid, according to a feedback control law that descends from duality-based methods applied to the optimal reactive power flow problem subject to power constraints. Convergence of the algorithm to the configuration of minimum losses and feasible voltages is proved analytically for both a synchronous and an asynchronous version of the algorithm, where agents update their state independently one from the other. Simulations are provided in order to illustrate the algorithm behavior, and the innovative feedback nature of such strategy is discussed.

I. INTRODUCTION

Recent technological advances, together with environmental and economic challenges, have been motivating the deployment of small power generators in the low voltage and medium voltage power distribution grid. The availability of a large number of these generators in the distribution grid can yield relevant benefits to the network operation: they can be used to provide a number of ancillary services that are of great interest for the management of the grid [1], [2]. In particular, many inverters have the capability, when they are running below their rated output current, to inject (or to absorb) reactive power together with active power [3]. With respect to the traditional devices, such as shunt capacitor banks or on-load tap changers [4], the inverters can act in the grid on a fast timescale. These abilities become necessary to exploit the advanced control capability of inverter interfaces to the grid. We focus on the problem of optimal reactive power compensation for power losses minimization, in presence of constraints in the reactive power inverters generation capabilities. In order to properly command the operation of these devices, the distribution network operator is required to solve an *optimal reactive power flow* (ORPF) problem. Powerful solvers have been designed for the ORPF problem, and advanced optimization techniques have been recently specialized for this task [5], [6]. However, these solvers assume that an accurate model of the grid is available, that all the grid buses are monitored, that loads announce their demand profiles in advance, and

that generators and actuators can be dispatched on a day-ahead, hour-ahead, and real-time basis. For this reason, these solvers are in general offline and centralized. These tools cannot be applied directly to the ORPF problem faced in microgrids and, more in general, in low/medium voltage power distribution networks, mainly because not all the buses of the grid are monitored, individual loads are unlikely to announce their demand profile in advance, the availability of small size generators is hard to predict. Moreover, the grid parameters, and sometimes even the topology of the grid, are only partially known, and generators are expected to connect and disconnect, requiring an automatic reconfiguration of the grid control infrastructure (the *plug and play* approach).

Only recently, algorithms that are truly scalable in the number of generators and do not require the monitoring of all the buses of the grid, have been proposed for the problem of power loss minimization, as [7] and [8]. While these algorithms have been designed by specializing classical nonlinear optimization algorithms to the ORPF problem, they can also be considered as *feedback* control strategies. Indeed, the key feature of these algorithms is that they require the alternation of measurement and actuation based on the measured data, and therefore they are inherently online algorithms. In particular, the reactive power injection of the generators is adjusted by these algorithms based on the phasorial voltage measurements that are performed at the buses where the generators are connected. The resulting closed loop system features a tight dynamic interconnection of the *physical layer* (the grid, the generators, the loads) with the *cyber layer* (where communication, computation, and decision happen). In this paper, we design a distributed feedback algorithm for the ORPF problem, in which the goal is to minimize reactive power flows when the microgenerators have limited generation capabilities.

In Section III, a model for the cyber-physical system of a smart power distribution grid is provided. In Section IV, the optimal reactive power flow problem with power constraints is stated. An algorithm for its solution is derived in Section V, by using the tools of dual decomposition. A synchronous and an asynchronous version of the algorithm are presented in Section VI. The convergence of both the proposed algorithms is studied in Section VII. Some simulations are provided in Section VIII.

II. MATHEMATICAL PRELIMINARIES AND NOTATION

Let $\mathcal{G} = (\mathcal{V}, \mathcal{E}, \sigma, \tau)$ be a directed graph, where \mathcal{V} is the set of nodes, \mathcal{E} is the set of edges, with $n = |\mathcal{V}|$, $r = |\mathcal{E}|$. Moreover $\sigma, \tau : \mathcal{E} \rightarrow \mathcal{V}$ are two functions such that edge

The authors are with the Dept. of Information Engineering, University of Padova, Via Gradenigo 6/a, 35131 Padova, Italy. Email: {saverio.bolognani, carlirug, cavraro, zampieri}@dei.unipd.it.

$e \in \mathcal{E}$ goes from the source node $\sigma(e)$ to the terminal node $\tau(e)$.

Given two nodes of the graph $h, k \in \mathcal{V}$, we define the path $\mathcal{P}_{hk} = (v_1, \dots, v_\ell)$ as the sequence of nodes, without repetitions, such that

- $v_1 = h$
- $v_\ell = k$
- for each $i = 1, \dots, \ell - 1$, the nodes v_i and v_{i+1} are connected by an edge (regardless of its direction).

In the rest of the paper we will often introduce complex-valued functions defined on the nodes and on the edges. These functions will also be intended as vectors in \mathbb{C}^n and \mathbb{C}^r . Given a vector u , we denote by \bar{u} its (element-wise) complex conjugate, and by u^T its transpose. We denote by $\Re(u)$ and by $\Im(u)$ the real and the imaginary part of u , respectively.

Let $A \in \{0, \pm 1\}^{r \times n}$ be the incidence matrix of the graph \mathcal{G} , defined via its elements

$$[A]_{ev} = \begin{cases} -1 & \text{if } v = \sigma(e) \\ 1 & \text{if } v = \tau(e) \\ 0 & \text{otherwise.} \end{cases}$$

If the graph \mathcal{G} is connected (i.e. for every pair of nodes there is a path connecting them), then $\mathbf{1}$ is the only vector in the null space $\ker A$, $\mathbf{1}$ being the column vector of all ones. We define by $\mathbf{1}_v$ the vector whose value is 1 in position v , and 0 everywhere else.

Given $u, v \in \mathbb{R}^\ell$, we define the operator $\text{proj}(u, v)$ as the component wise projection of u in the set $\{w \in \mathbb{R}^\ell : w_h \leq v_h, h = 1, \dots, \ell\}$, that is,

$$(\text{proj}(u, v))_h = \begin{cases} u_h & \text{if } u_h \leq v_h \\ v_h & \text{if } u_h > v_h \end{cases} \quad (1)$$

III. CYBER-PHYSICAL MODEL OF A SMART POWER DISTRIBUTION GRID

In this work, we envision a *smart* power distribution network as a cyber-physical system, in which

- the **physical layer** consists of the power distribution infrastructure, including power lines, loads, microgenerators, and the point of connection to the transmission grid, while
- the **cyber layer** consists of intelligent agents, dispersed in the grid, and provided with actuation, sensing, communication, and computational capabilities.

A. Physical layer

For the purpose of this paper, we model the physical layer as a directed graph \mathcal{G} , in which edges in \mathcal{E} represent the power lines, and nodes in \mathcal{V} represent both loads and generators that are connected to the microgrid (see Figure 1, middle panel). These include the residential and industrial consumers, microgenerators, and also the point of connection of the microgrid to the transmission grid (called point of common coupling, or PCC).

We limit our study to the steady state behavior of the system, where all voltages and currents are sinusoidal signals at the same pulsation ω_0 . Each signal can therefore be

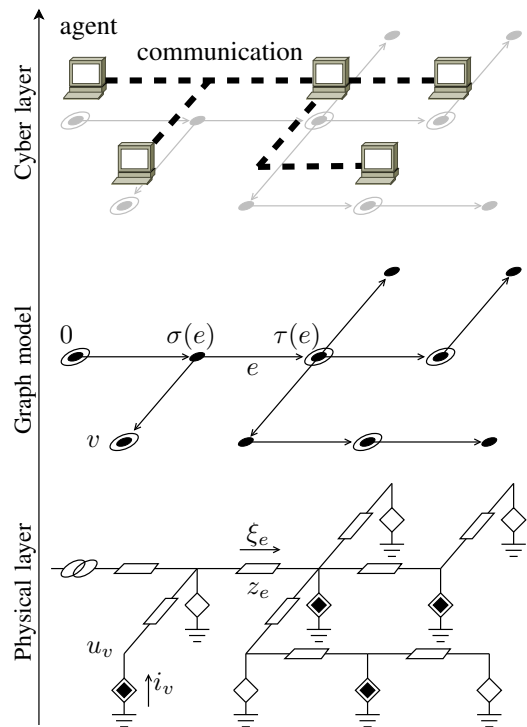


Fig. 1. Schematic representation of the microgrid model. In the lower panel the physical layer is represented via a circuit representation, where black diamonds are microgenerators, white diamonds are loads, and the left-most element of the circuit represents the PCC. The middle panel illustrates the adopted graph representation for the same grid. Circled nodes represent both microgenerators and the PCC. The upper panel represents the cyber layer, where agents (i.e. microgenerator nodes and the PCC) are also connected via some communication infrastructure.

represented via a complex number whose amplitude corresponds to the signal root-mean-square value, and whose phase corresponds to the phase of the signal with respect to an arbitrary global reference. Therefore, y represents the signal $y(t) = |y|\sqrt{2}\sin(\omega_0 t + \angle y)$. The system state is described by the following system variables (see Figure 1, lower panel):

- $u \in \mathbb{C}^n$, where u_v is the grid voltage at node v ;
- $i \in \mathbb{C}^n$, where i_v is the current injected by node v into the grid;
- $\xi \in \mathbb{C}^r$, where ξ_e is the current flowing on edge e .
- $s = p + iq \in \mathbb{C}^r$, where s_v, p_v and q_v are the complex, the active and the reactive power injected by node v into the grid respectively;

For every edge e of the graph, we define by z_e the impedance of the corresponding power line. We assume the following.

Assumption 1: All power lines in the grid have the same inductance/resistance ratio, i.e.

$$z_e = e^{j\theta} |z_e|$$

for any e in \mathcal{E} and for a fixed θ .

This assumption is satisfied when the grid is relatively homogeneous, and is reasonable in most practical cases (see for example the IEEE standard testbeds [9]). The following equations (Kirchhoff's current and voltage law) are satisfied

by u, i and ξ :

$$A^T \xi + i = 0, \quad (2)$$

$$Au + e^{i\theta} Z \xi = 0, \quad (3)$$

with $Z = \text{diag}(|z_e|, e \in \mathcal{E})$. From (2) and (3) we can also obtain

$$i = e^{-j\theta} Lu \quad (4)$$

where L is the weighted Laplacian of the graph $L := A^T Z^{-1} A$.

Each node v of the grid is also characterized by a law relating its injected current i_v with its voltage u_v . We label the PCC as node 0 and take it as an ideal sinusoidal voltage generator (called *slack bus* in the power system analysis terminology) at the microgrid nominal voltage U_N with arbitrary, but fixed, angle ϕ

$$u_0 = U_N e^{i\phi}. \quad (5)$$

We model loads and microgenerators (that is, every node v of the microgrid except the PCC) via the following law relating the voltage u_v and the current i_v

$$u_v \bar{i}_v = s_v, \quad \forall v \in \mathcal{V} \setminus \{0\}. \quad (6)$$

The complex powers s_v corresponding to grid loads are such that $\{p_v < 0\}$, meaning that positive active power is *supplied* to the devices. The complex powers corresponding to microgenerators, on the other hand, are such that $\{p_v \geq 0\}$, as positive active power is *injected* into the grid. In the power system analysis terminology, all nodes but the PCC are being modeled as *constant power* or *P-Q buses*. Microgenerators fit in this model, as they generally are commanded via a complex power reference and they can inject it independently from the voltage at their point of connection [10], [11].

B. Cyber layer

We assume that every microgenerator, and also the PCC, correspond to an *agent* in the cyber layer (see the upper panel of Figure 1). We denote by \mathcal{C} (with $|\mathcal{C}| = m$) this subset of the nodes of \mathcal{G} .

Each agent is provided with some computational capability, and with some sensing capability, in the form of a phasor measurement unit (i.e. a sensor that can measure voltage amplitude and angle [12]). Agents that corresponds to a microgenerator can also actuate the system, by commanding the amount of reactive power injected by that microgenerator.

Finally, agents can communicate, via some communication channel that could possibly be the same power lines (via power line communication – PLC – technology). Motivated by this possibility, we define the neighbors in the cyber layer in the following way.

Definition 2 (Neighbors in the cyber layer): Let $h \in \mathcal{C}$ be an agent of the cyber layer. The set of agents that are neighbors of h in the cyber layer, denoted as $\mathcal{N}(h)$, is the subset of \mathcal{C} defined as

$$\mathcal{N}(h) = \{k \in \mathcal{C} \mid \forall \mathcal{P}_{hk}, \mathcal{P}_{hk} \cap \mathcal{C} = \{h, k\}\}.$$

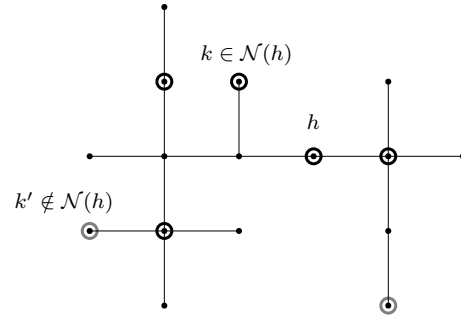


Fig. 2. An example of neighbor agents in the cyber layer. Circled nodes (both gray and black) are agents (nodes in \mathcal{C}). Nodes circled in black belong to the set $\mathcal{N}(h) \subset \mathcal{C}$. Node circled in gray are agents which do not belong to the set of neighbors of h . For each agent $k \in \mathcal{N}(h)$, the path that connects h to k does not include any other agent besides h and k themselves.

Figure 2 gives an example of such set.

We assume that every agent $h \in \mathcal{C}$ knows its set of neighbors $\mathcal{N}(h)$, and can communicate with them. Notice that this architecture can be constructed by each agent in a distributed way, for example by exploiting the PLC channel (as suggested for example in [13]). This allows also a plug-and-play reconfiguration of such architecture when new agents are connected to the grid.

IV. OPTIMAL REACTIVE POWER FLOW PROBLEM

We consider the problem of commanding the reactive power injection of the microgenerators in order to minimize power distribution losses on the power lines, taking into account the limited generation capability of each microgenerator. The decision variables are the reactive power commands $q_h, h \in \mathcal{C} \setminus \{0\}$.

Power distribution losses can be expressed, by using (3), as

$$J_{\text{losses}} := \sum_{e \in \mathcal{E}} |\xi_e|^2 \Re(z_e) = \bar{u}^T L u. \quad (7)$$

Given an upper bound $q_v^{max} \in \mathbb{C}^{m-1}$ (where q_v^{max} represents the maximum amount of reactive power that the v -th compensator can inject into the grid), we can therefore formulate the following optimization problem,

$$\min_{q_h, h \in \mathcal{C} \setminus \{0\}} \bar{u}^T L u \quad (8a)$$

$$\text{subject to } q_h \leq q_h^{max}, \quad \forall h \in \mathcal{C} \setminus \{0\} \quad (8b)$$

While we are not considering lower bounds on the bus voltage magnitudes, in the form $q_h \geq q^{min}$, they could be easily incorporated with minor modifications of the algorithm, at the cost of a slightly more complex notation.

In order to adopt a compact notation for the system inputs, measured outputs, and state, we introduce the following block decomposition of the vector of voltages u

$$u = \begin{bmatrix} u_0 \\ u_G \\ u_L \end{bmatrix},$$

where u_0 is the voltage at the PCC, $u_G \in \mathbb{C}^{m-1}$ are the voltages at the microgenerators, and $u_L \in \mathbb{C}^{n-m}$ are the voltages at the loads. Similarly, we also define $s_G = p_G + jq_G$ and $s_L = p_L + jq_L$.

From a system-wide perspective, the control problem that we are considering is therefore characterized by

- the input variables q_G ,
- the measured output variables $\begin{bmatrix} u_0 \\ u_G \end{bmatrix}$,
- the unmeasured disturbances p_L, q_L, p_G .

Remark 3: While the decision variables of the ORPF problem (i.e. the input variables q_G) do not include the reactive power provided to the distribution grid by the PCC (i.e. $q_0 = u_0 \bar{i}_0$), this quantity will also change every time the reactive power injections of the generators are updated by the algorithm, because the inherent physical behavior of the slack bus (the PCC) ensures that equations (4), (5) and (6) are automatically satisfied at every time.

V. A MODIFIED DUAL ALGORITHM

In this section, in order to derive a control strategy to solve the ORPF problem, we apply the tool of dual decomposition to (8). While problem (8) might not be convex in general, we rely on the results presented in [14] which show that zero duality gap holds for the ORPF problems, under some conditions that are commonly verified in practice. Based on this result, we use an approximate explicit solution of the nonlinear equations (4), (5), and (6), to derive the a *dual ascent algorithm* [15] that can be implemented by the agents.

In order to present the approximate solution, we need the following technical lemma.

Lemma 4 (Lemma 1 in [8]): Let L be the weighted Laplacian of \mathcal{G} . There exists a unique symmetric, positive semidefinite matrix $X \in \mathbb{R}^{n \times n}$ such that

$$\begin{cases} XL = I - \mathbf{1}\mathbf{1}_0^T \\ X\mathbf{1}_0 = 0. \end{cases} \quad (9)$$

The matrix X depends only on the topology of the grid power lines and on their impedance (compare it with the definition of Green matrix in [16]). Notice that, if the grid is radial (i.e. \mathcal{G} is a tree) then Z_{hk}^{eff} is simply the impedance of the only path from node h to node k .

By adopting the same block decomposition as before, we have

$$X = \begin{bmatrix} 0 & 0 & 0 \\ 0 & M & N \\ 0 & N^T & O \end{bmatrix}, \quad (10)$$

with $M \in \mathbb{R}^{(m-1) \times (m-1)}$, $N \in \mathbb{R}^{(m-1) \times (m-n)}$, and $O \in \mathbb{R}^{(n-m) \times (n-m)}$. The following proposition provides the approximate relation between the grid voltages and the power injections at the nodes.

Proposition 5: Consider the physical model described by the set of nonlinear equations (2), (3), (5), and (6). Node voltages then satisfy

$$\begin{bmatrix} u_0 \\ u_G \\ u_L \end{bmatrix} = e^{j\phi} \left(U_N \mathbf{1} + \frac{e^{j\theta}}{U_N} \begin{bmatrix} 0 & 0 & 0 \\ 0 & M & N \\ 0 & N^T & O \end{bmatrix} \begin{bmatrix} 0 \\ \bar{s}_G \\ \bar{s}_L \end{bmatrix} \right) + o\left(\frac{1}{U_N}\right), \quad (11)$$

where the little-o notation means that $\lim_{U_N \rightarrow \infty} \frac{o(f(U_N))}{f(U_N)} = 0$.

Proof: The proposition descends directly from Proposition 1 in [8]. ■

The quality of this approximation relies on having large nominal voltage U_N and relatively small currents injected by the inverters (or supplied to the loads). This assumption is verified in practice, and corresponds to correct design and operation of power distribution networks, where indeed the nominal voltage is chosen sufficiently large (subject to other functional constraints) in order to deliver electric power to the loads with relatively small power losses on the power lines. In [8], a brief discussion about how this approximation extends the DC power flow model [17, Chapter 3] to the lossy case, has been provided.

Given the approximate explicit expression for voltages u presented in Proposition 5, we can reformulate (8) as the approximate problem

$$\min_{q_h, h \in \mathcal{C} \setminus \{0\}} q_G^T \frac{M}{2} q_G + q_G^T N q_L \quad (12a)$$

$$\text{subject to } q_h \leq q_h^{\text{max}}, \quad \forall h \in \mathcal{C} \setminus \{0\} \quad (12b)$$

We proceed by proposing a dual-ascent like algorithm which guarantees that the constraints $q_h \leq q_h^{\text{max}}$, $\forall h \in \mathcal{C} \setminus \{0\}$ are guaranteed at each iteration. To do so let us introduce the Lagrangian associated to (12)

$$\mathcal{L}(q_G, \lambda) = q_G^T \frac{M}{2} q_G + q_G^T N q_L + \lambda^T (q - q^{\text{max}}) \quad (13)$$

Our dual ascent algorithm consists in the iterative execution of the following alternated steps:

- 1) computation of the minimum w.r.t. the primal variable q_G

$$\bar{q}_G = \arg \min_{q_G} \mathcal{L}(q_G, \lambda(t)), \quad (14)$$

- 2) update of the Lagrange multipliers update

$$\lambda(t+1) = \left[\lambda(t) + \gamma \frac{\partial \mathcal{L}(\bar{q}, \lambda(t))}{\partial \lambda} \right]_+, \quad (15)$$

- 3) actuation of \bar{q}_G projected in the feasible set

$$q_G(t+1) = \text{proj}(\bar{q}_G, q^{\text{max}}) \quad (16)$$

where the $[\cdot]_+$ operator corresponds to the projection on the positive orthant and γ is a suitable positive constant.

Notice that the above algorithm differs from the standard dual ascent algorithm that would be

$$q_G(t+1) = \arg \min_{q_G} \mathcal{L}(q_G, \lambda(t)), \quad (17)$$

$$\lambda(t+1) = \left[\lambda(t) + \gamma \frac{\partial \mathcal{L}(q_G(t+1), \lambda(t))}{\partial \lambda} \right]_+, \quad (18)$$

It is well known that algorithm defined in (17) and (18) converges to the optimal solution of problem in (12a) and (12b) (see [15]), even though the constraints (12b) are guaranteed to be satisfied only asymptotically, namely, there might be some iterations where $q_h(t) > q_h^{\text{max}}$. Instead, due to the limited generation capabilities of the micro-generators,

we need (12b) to be satisfied at each iteration and this fact is guaranteed by (16).

However it is worth stressing that algorithm in (14), (15), (16) and algorithm in (17), (18), generate the same trajectory for the Lagrange multipliers λ , when starting from the same initial conditions. This fact is formally stated in the next Proposition.

Proposition 6: Let q_G, λ be the primal variable and the dual variable, respectively, of algorithm in (14), (15), (16). Let $\tilde{q}_G, \tilde{\lambda}$ be the primal variable and the dual variable, respectively, of algorithm in (17), (18). Assume $q_G(0) = \tilde{q}_G(0)$ and $\lambda(0) = \tilde{\lambda}(0)$. Then $\lambda(t) = \tilde{\lambda}(t)$ for all $t \geq 0$.

Proof: It is straightforward to see that the minimization of (14) and (17) is achieved by

$$\bar{q}_G = q_G(t+1) = -M^{-1}(Nq_L + \lambda(t)) \quad (19)$$

Notice that $\bar{q} = q_G(t+1)$ depends only on the multiplier $\lambda(t)$ and q_L , while it is independent from $q_G(t)$. It follows that the dual variable updates (15) and (18) have the same form

$$\lambda(t+1) = \left[(I - \gamma M^{-1}) \lambda(t) - \gamma M^{-1} N q_L - q^{max} \right]_+ \quad (20)$$

which is independent from the primal variable value, and so the evolution of λ in (15) and (18) is identical. ■

The previous proposition justifies, in some sense, the use of our modified algorithm. Indeed the main consequence of Proposition 6 is that both algorithm in (14), (15), (16) and algorithm in (17) and (18) converge asymptotically to the same dual optimal solution. It turns out that the primal variable of algorithm in (14), (15), (16), whose feasibility is guaranteed by the projection (16), converges asymptotically to the optimal primal solution of (17).

Corollary 7: Let q_G, λ be the primal variable and the dual variable, respectively, of algorithm in (14), (15), (16). Let $\tilde{q}_G, \tilde{\lambda}$ be the primal variable and the dual variable, respectively, of algorithm in (17), (18). We have then that q_G and \tilde{q}_G converge asymptotically to the same optimal value.

VI. SYNCHRONOUS AND ASYNCHRONOUS ALGORITHM

In this section, we show how the agents can implement the algorithm proposed in in (14), (15), (16). In order to derive the update law for the agents, we need to introduce the following matrix G .

Lemma 8: There exists a unique symmetric matrix $G \in \mathbb{R}^{m \times m}$ such that

$$\begin{cases} \begin{bmatrix} 0 & 0 \\ 0 & M \end{bmatrix} G = I - \mathbf{1}\mathbf{1}_0^T \\ G\mathbf{1} = 0. \end{cases}$$

Proof: The following symmetric matrix G satisfies the conditions.

$$G = \begin{bmatrix} \mathbf{1}^T M^{-1} \mathbf{1} & -\mathbf{1}^T M^{-1} \\ -M^{-1} \mathbf{1} & M^{-1} \end{bmatrix}. \quad (21)$$

The proof of uniqueness, that we omit here, follows exactly the same steps as in the proof of Lemma 4. ■

The matrix G has also a remarkable sparsity pattern, as the following lemma states.

Lemma 9: The matrix G has the sparsity pattern induced by the Definition 2 of neighbor agents in the cyber layer, i.e.

$$G_{hk} \neq 0 \Leftrightarrow k \in \mathcal{N}(h).$$

The proof is provided in [18], where it is also discussed how the elements of G can be estimated by the agents, given a local knowledge of the power grid topology and parameters.

We therefore propose the following synchronous algorithm, assuming that the agents are coordinated, i.e. they can update their state variables q_h and λ_h , $h \in \mathcal{C} \setminus \{0\}$, synchronously.

Let all agents store an auxiliary scalar variable λ_h (for the PCC, $\lambda_0 = 0$). Let γ be a positive scalar parameter, and let θ be the impedance angle defined in Assumption 1. Let G_{hk} be the elements of the matrix G defined in Lemma 8. At every synchronous iteration of the algorithm, each agent $h \in \mathcal{C} \setminus \{0\}$ executes the following operations in order:

- 1) gathers the voltage measurements

$$\{u_k = |u_k| \exp(j\angle u_k), k \in \mathcal{N}(h)\}$$

- and the Lagrange multipliers λ_k from its neighbors;
- 2) computes the optimal reactive power q_h regardless the generation capability as

$$\begin{aligned} q_h &\leftarrow q_h + \\ &+ \sum_{k \in \mathcal{N}(h)} G_{hk} (|u_h| |u_k| \sin(\angle u_k - \angle u_h - \theta) - \lambda_k). \end{aligned} \quad (22)$$

- 3) updates the auxiliary variable λ_h as

$$\lambda_h \leftarrow [\lambda_h + \gamma(q_h - q_h^{max})]_+; \quad (23)$$

- 4) projects q_h into the feasible region, i.e.,

$$q_h \leftarrow \text{proj}(q_h, q_h^{max}) \quad (24)$$

and actuates this projected value of q_h .

It can be shown, by using Lemma 9 and via some algebraic manipulations, that the update (22) can be also rewritten as

$$q_G \leftarrow q_G(t) - M^{-1} \lambda(t) + \Im \left(e^{-j\theta} [0 \quad \text{diag}(\bar{u}_G)] G \begin{bmatrix} u_0 \\ u_G \end{bmatrix} \right),$$

which, by using the expression for u provided by Proposition 5, is equal to

$$q_G \leftarrow -M^{-1}(\lambda + Nq_L) + o\left(\frac{1}{U_N}\right).$$

It turns out that

$$\frac{\partial \mathcal{L}(q_G, \lambda)}{\partial q_G} = o\left(\frac{1}{U_N}\right),$$

namely, q_G minimizes the Lagrangian with respect to the primal variables, up to a term that vanishes for large U_N . It

follows that the the update in (22) is equivalent to the update in (14).

In order to avoid the burden of coordination among the agents, we also propose an asynchronous version of the algorithm, in which the agents corresponding to the micro-generators update their state (q_h, λ_h) independently one from the other, based on the information that they can measure and that they can gather from their neighbors.

We assume that each agent (except for the agent located at the PCC) is provided with an individual timer, by which it is triggered. Timers tick randomly, with exponentially, identically distributed waiting times. When an agent is triggered, it gathers the voltage measurements $\{u_k = |u_k| \exp(j\angle u_k), k \in \mathcal{N}(h)\}$ from its neighbors, and then executes the operations explained in (22), (23) and (24), while the dual and the primal variable of all the other agents are kept fixed. Observe that the update equations for the asynchronous algorithm are exactly the same of the synchronous case. However, each agent updates its primal and dual variables asynchronously and independently from all the other agents.

VII. CONVERGENCE ANALYSIS

In this section, we study the convergence of both the synchronous and of the asynchronous algorithm. For the analysis of the stability of both of them, we adopt again the approximated model proposed in Proposition 5, and we neglect the infinitesimal terms. Thanks to 7, for the synchronous case we can study the convergence of the algorithm (17) and (18) instead of the one of (14) and (15). We then consider the update equations

$$q_G(t+1) = -M^{-1}(Nq_L + \lambda(t)). \quad (25)$$

for the primal variables, and

$$\lambda(t+1) = [\lambda(t) + \gamma(q_G(t+1) - q^{max})]_+, \quad (26)$$

for the dual variables.

Notice that the equilibrium (q_G^*, λ^*) of (26)-(25) is characterized by

$$q_G^* - q^{max} \leq 0 \quad \text{and} \quad q_G^* + M^{-1}(Nq_L + \lambda^*) = 0,$$

and therefore we have that

$$\frac{\partial \mathcal{L}(q_G^*, \lambda^*)}{\partial q_G^*} = 0,$$

which correspond to the necessary conditions for the optimality of (q_G^*, λ^*) according to Uzawa's saddle point theorem [19]. The following convergence result holds.

Theorem 10 (Synchronous case): Consider the dynamic system described by the update equations (25) and (26). The equilibrium (q^*, λ^*) is asymptotically stable if

$$\gamma \leq \frac{2}{\rho(M^{-1})},$$

where $\rho(M^{-1})$ is the M^{-1} spectral radius.

Proof: While we are considering the algorithm (17) and (18), it is straightforward to compute the dual function $g(\lambda) = \min_{q_G} \mathcal{L}(q_G, \lambda)$ and state the dual problem

$$\max_{\lambda \geq 0} \mathcal{L}(q_G, \lambda). \quad (27)$$

If $\gamma \leq \frac{2}{\rho(M^{-1})}$, (27) is guaranteed to converge to the optimal solution of (12) (see [20], Proposition 3.4). ■

For the asynchronous case, on the other hand, we introduce the following assumption.

Assumption 11: Let $\{T_i^{(h)}\}, i \in \mathbb{N}$, be the time instants in which the agent h is triggered by its own timer. We assume that the timer ticks with exponentially distributed waiting times, identically distributed for all the agents in $\mathcal{C} \setminus \{0\}$.

Let us define the random sequence $h(t) \in \mathcal{C} \setminus \{0\}$ which tells which agent has been triggered at iteration t of the algorithm. Because of Assumption 11, the random process $h(t)$ is an i.i.d. uniform process on the alphabet $\mathcal{C} \setminus \{0\}$. We therefore consider the following update equations, in which only the component $h(t)$ of the vectors q_G and λ is updated at time t :

$$\begin{cases} \bar{q}_{h(t)}(t+1) = -\mathbf{1}_{h(t)}^T M^{-1}(Nq_L + \lambda(t)) \\ q_k(t+1) = q_k(t) \quad \text{for all } k \neq h(t). \end{cases} \quad (28)$$

$$\begin{cases} \lambda_{h(t)}(t+1) = [\lambda_{h(t)}(t) + \gamma(\bar{q}_{h(t)}(t+1) - q_{h(t)}^{max})]_+ \\ \lambda_k(t+1) = \lambda_k(t) \quad \text{for all } k \neq h(t), \end{cases} \quad (29)$$

and finally

$$\begin{cases} q_{h(t)}(t+1) = \text{proj}(\bar{q}_{h(t)}(t+1), q_{h(t)}^{max}) \\ q_k(t+1) = q_k(t) \quad \text{for all } k \neq h(t). \end{cases} \quad (30)$$

Notice that, also in the asynchronous case, Uzawa's necessary conditions for optimality are satisfied at the equilibrium of (29)-(28).

The following convergence result holds.

Theorem 12 (Asynchronous case): Consider the dynamic system described by the update equations (29), (28) and (30). Let Assumption 11 hold. Then the evolution $t \rightarrow (q(t), \lambda(t))$ converges almost surely to the equilibrium (q^*, λ^*) if

$$\gamma \leq \frac{2}{\rho(M^{-1})},$$

where $\rho(M^{-1})$ is the M^{-1} spectral radius.

The proof is presented in Appendix .

VIII. SIMULATIONS

The algorithm has been tested on the testbed IEEE 37 [9], which is an actual portion of 4.8kV power distribution network located in California. The load buses are a blend of constant-power, constant-current, and constant-impedance loads, with a total power demand of almost 2 MW of active power and 1 MVAR of reactive power (see [9] for the testbed data). The length of the power lines range from a minimum of 25 meters to a maximum of almost 600 meters. The impedance of the power lines differs from edge to edge, however, the inductance/resistance ratio exhibits a smaller

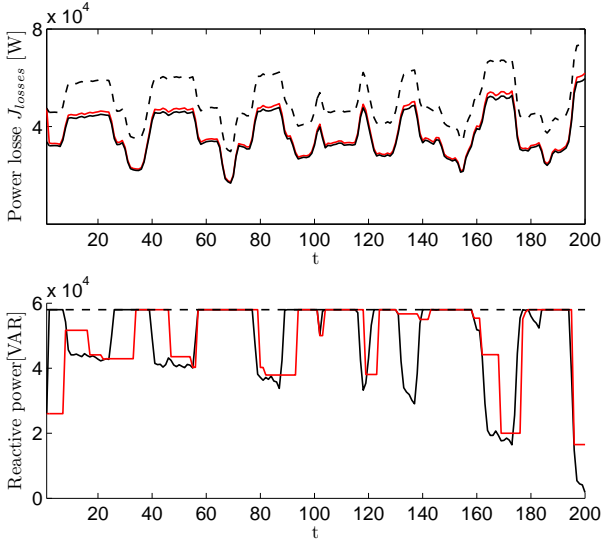


Fig. 3. In the upper panel we have the power distribution losses for the following cases: with no reactive power compensation (dashed line), when an ideal centralized numerical controller commands the microgenerators (thick black line), and for the proposed algorithm, where microgenerators are commanded via a feedback law from the voltage measurements (thin red line). In the lower panel we have the reactive power injected by a generator both in the synchronous (black line) and in the asynchronous case (red line), together with the maximum amount of injectable reactive power (dashed line).

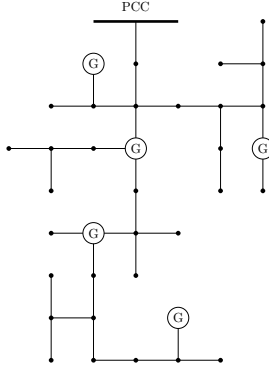


Fig. 4. Schematic representation of the IEEE 37 test feeder [9], where 5 microgenerators have been deployed.

variation, ranging from $\angle z_e = 0.47$ to $\angle z_e = 0.59$. This justifies Assumption 1. We considered the scenario in which 5 microgenerators have been deployed in this portion of the power distribution grid (see Figure 4).

The maximum reactive power capabilities of each generator has been set to values that go from 14 kVAR to 200 kVAR. Both the synchronous and the asynchronous algorithm presented in Section VI have been simulated on a nonlinear exact solver of the grid [21]. The approximate model presented in Proposition 5 has not been used in these simulations, being only a tool for the design of the algorithm and for the study of the algorithm's convergence. The parameter γ has been chosen as one half of the bound indicated by Theorem 10 and Theorem 12 for convergence. Timers in the asynchronous case have been tuned so that each agent is triggered, in expectation, at the same rate of the synchronous case.

A time-varying profile for the loads has been generated,

in order to simulate the effect of slowly varying loads (e.g. the aggregate demand of a residential neighborhood), fast changing demands (e.g. some industrial loads), and intermittent large loads (e.g. heating).

The results of the simulation have been plotted in Figure 3. In the upper panel represents, the power distribution losses are reported. The dashed line represents the case in which no reactive power compensation is performed, the thick black line represents the best possible strategy that solves the ORPF problem (8) (computed via a numerical centralized solver that have access to all the grid parameters and load data) and the thin red line represents the behavior of the proposed asynchronous algorithm. The behavior of the synchronous algorithm is here omitted for the sake of clearness, being almost identical to the one of the asynchronous algorithm. In the lower panel are reported the trajectories of the reactive power injected by a compensator both in the synchronous or in the asynchronous case. Notice that they are always within the feasible region.

It can be seen that the proposed algorithm achieves practically the same performance of the centralized solver, in terms of power distribution losses. Notice however that it does not have access to the demands of the loads, which are unmonitored. The agents, located only at the microgenerators, can only access their voltage measurements and share them with their neighbors.

APPENDIX

Proof of Theorem 12

Proof: [Proof of Theorem 12] Let (q_G^*, λ^*) be the equilibrium of the system (26)-(25), which satisfies the following equations

$$\sin \theta \lambda^* - (q_G^* + M^{-1} N q_L) = 0 \quad (31a)$$

$$q - q^{max} \leq 0 \quad \forall h \in \mathcal{C} \quad (31b)$$

$$q - q^{max} < 0 \quad \Leftrightarrow \quad \lambda_h^* = 0.. \quad (31c)$$

We introduce the following quantities

$$x(t) = q_G(t) - q_G^*, \quad \bar{x}(t) = \bar{q}_G(t) - q_G^* \quad \text{and} \quad y(t) = \lambda(t) - \lambda^*.$$

Consider the update equations (28), (29) and (30). We can write, assuming, without loss of generality, that node h is the node performing the update at the t -th iteration

$$\begin{aligned} \bar{x}_h(t+1) &= \\ &= -\mathbf{1}_h^T M^{-1} (N q_L + \lambda(t)) - q_h^* \\ &= -\mathbf{1}_h^T M^{-1} y(t) - \mathbf{1}_h^T (q_h^* + M^{-1} (N q_L + \lambda^*)) \\ &= -\mathbf{1}_h^T M^{-1} y(t) \end{aligned}$$

exploiting (31a).

As far as the variable y is concerned we have that

$$\begin{aligned} y_h(t+1) &= \\ &= [\lambda_h(t) + \gamma (\bar{q}_h(t+1) - q_h^{max})]_+ - [\lambda_h^*]_+ \\ &= [y_h(t) + \gamma \bar{x}_h(t+1) + \lambda_h^* + \gamma (q_h^* - q_h^{max})]_+ - [\lambda_h^*]_+. \end{aligned}$$

Finally we have

$$x(t+1) = \text{proj}(\bar{x}, q^{max} - q^*) \quad (32)$$

Let $\alpha_h = \lambda_h^* + \gamma(q_h^* - q_h^{max})$ and observe that $[\lambda_h^*]_+ = [\alpha_h]_+$. Hence we can write

$$y_h(t+1) = [y_h(t) + \gamma \bar{x}_h(t+1) + \alpha_h]_+ - [\alpha_h]_+$$

Observe that Assumption 11 implies there exists almost surely a positive integer T such that any node has performed an update within the window $[0, T]$. It follows that, for $t \geq T$

$$\bar{x}(t+1) = -M^{-1}y(t). \quad (33)$$

Accordingly for $t \geq T$ the update for y can be rewritten as

$$y_h(t+1) = [(I - \gamma M^{-1})y_h(t) + \alpha_h]_+ - [\alpha_h]_+$$

and, clearly, $y_k(t+1) = y_k(t)$, for $k \neq h$.

Now let $P_h = I - \gamma \mathbf{1}_h \mathbf{1}_h^T M^{-1}$. By using the fact that $\|a_+ - b_+\| \leq \|a - b\|$, it follows

$$\|y(t+1)\| \leq \|P_h y(t)\|.$$

Consider the evolution of the quantity $\mathbb{E}[\|y(t)\|^2]$. From the above inequality we get that

$$\begin{aligned} \mathbb{E}[\|y(t+1)\|^2] &\leq \mathbb{E}[y(t)^T P_h^T P_h y(t)] \\ &= \text{trace} \mathbb{E}[y(t)^T P_h^T P_h y(t)] \\ &= \text{trace} \{ \mathbb{E}[P_h^T P_h y(t) y(t)^T] \} \\ &\leq \| \mathbb{E}[P_h^T P_h] \| \text{trace} \{ \mathbb{E}[y(t) y(t)^T] \} \\ &\leq \| \mathbb{E}[P_h^T P_h] \| \mathbb{E}[\|y(t)\|^2] \end{aligned} \quad (34)$$

where, given two semidefinite matrices A, B , we used the fact that $\text{trace}\{AB\} \leq \|A\| \text{trace}\{B\}$. Let us compute $\mathbb{E}[P_h^T P_h]$. Observe that

$$P_h^T P_h = I - \gamma(M^{-1} \mathbf{1}_h \mathbf{1}_h^T + \mathbf{1}_h \mathbf{1}_h^T M^{-1}) + \gamma^2 M^{-1} \mathbf{1}_h \mathbf{1}_h^T M^{-1}$$

from which we get, by using Assumption 11,

$$\begin{aligned} \mathbb{E}[P_h^T P_h] &= \frac{1}{m-1} \sum P_h^T P_h \\ &= I - \gamma \frac{M^{-1}}{m-1} + \gamma^2 \frac{(M^{-1})^2}{m-1}. \end{aligned}$$

One can see that if the spectral radius of the above matrix is smaller than one, i.e. it holds

$$\gamma < \frac{2}{\rho(M^{-1})}, \quad (35)$$

y converges to zero, and therefore, from (32) and (33), also \bar{x} and x converge to zero. The proof can be concluded by invoking the Supermartingale Convergence Theorem [22]. For the sake of the clarity, we recall that this theorem states that, if X_t , $t \geq 0$, is a nonnegative random variable such that $\mathbb{E}[X_1] < +\infty$ and if $\mathbb{E}[X_{t+1} | \mathcal{F}_t] \leq X_t$ with probability one, where \mathcal{F}_t denotes the history of the process X_t up to time t , then X_t tends to a limit X with probability one, and $\lim_{t \rightarrow \infty} \mathbb{E}[X_t] = \mathbb{E}[X]$.

Let $X_t = \|y(t)\|^2$. Observe that

$$\begin{aligned} \mathbb{E}[\|y(t+1)\|^2 | y(t)] &\leq \mathbb{E}[y(t)^T P_h^T P_h y(t) | y(t)] \\ &\leq \| \mathbb{E}[P_h^T P_h] \| \|y(t)\|^2 \\ &\leq \|y(t)\|^2 \end{aligned}$$

where the last inequality follows from the fact that $\| \mathbb{E}[P_h^T P_h] \| < 1$ under condition (35). Moreover inequality (34) together with $\| \mathbb{E}[P_h^T P_h] \| < 1$ implies that $\lim_{t \rightarrow \infty} \mathbb{E}[\|y(t)\|^2] = 0$. Hence $\mathbb{E}[\|y(t)\|^2]$ converges with probability one to a nonnegative random variable X such that $\mathbb{E}[X] = 0$, i.e., X is the null random variable. This concludes the proof. \blacksquare

REFERENCES

- [1] F. Katiraei and M. R. Iravani, "Power management strategies for a microgrid with multiple distributed generation units," *IEEE Trans. Power Syst.*, vol. 21, no. 4, pp. 1821–1831, Nov. 2006.
- [2] M. Prodanovic, K. De Brabandere, J. Van den Keybus, T. Green, and J. Driesen, "Harmonic and reactive power compensation as ancillary services in inverter-based distributed generation," *IET Gener. Transm. Distrib.*, vol. 1, no. 3, pp. 432–438, 2007.
- [3] K. Turitsyn, P. Šulc, S. Backhaus, and M. Chertkov, "Options for control of reactive power by distributed photovoltaic generators," *Proc. IEEE*, vol. 99, no. 6, pp. 1063–1073, Jun. 2011.
- [4] M. E. Baran and F. F. Wu, "Optimal sizing of capacitors placed on a radial distribution system," *IEEE Trans. Power Del.*, vol. 4, no. 1, pp. 735–743, Jan. 1989.
- [5] B. Zhao, C. X. Guo, and Y. J. Cao, "A multiagent-based particle swarm optimization approach for optimal reactive power dispatch," *IEEE Trans. Power Syst.*, vol. 20, no. 2, pp. 1070–1078, May 2005.
- [6] J. Lavaei, A. Rantzer, and S. H. Low, "Power flow optimization using positive quadratic programming," in *Proc. 18th IFAC World Congr.*, 2011.
- [7] P. Tenti, A. Costabeber, P. Mattavelli, and D. Trombetti, "Distribution loss minimization by token ring control of power electronic interfaces in residential microgrids," *IEEE Trans. Ind. Electron.*, vol. 59, no. 10, pp. 3817–3826, Oct. 2012.
- [8] S. Bolognani and S. Zampieri, "A distributed control strategy for reactive power compensation in smart microgrids," *submitted to IEEE Transactions on Automatic Control*, 2012, arXiv preprint available [math.OA] 1106.5626.
- [9] W. H. Kersting, "Radial distribution test feeders," in *IEEE Power Engineering Society Winter Meeting*, vol. 2, Jan. 2001, pp. 908–912.
- [10] J. A. Lopes, C. L. Moreira, and A. G. Madureira, "Defining control strategies for microgrids islanded operation," *IEEE Trans. Power Syst.*, vol. 21, no. 2, pp. 916–924, May 2006.
- [11] T. C. Green and M. Prodanović, "Control of inverter-based microgrids," *Electr. Pow. Syst. Res.*, vol. 77, no. 9, pp. 1204–1213, Jul. 2007.
- [12] A. G. Phadke, "Synchronized phasor measurements in power systems," *IEEE Comput. Appl. Power*, vol. 6, no. 2, pp. 10–15, Apr. 1993.
- [13] A. Costabeber, T. Erseghe, P. Tenti, S. Tomasin, and P. Mattavelli, "Optimization of micro-grid operation by dynamic grid mapping and token ring control," in *Proc. 14th European Conf. on Power Electronics and Applications (EPE)*, Birmingham, UK, 2011.
- [14] J. Lavaei and S. H. Low, "Zero duality gap in optimal power flow problem," *IEEE Trans. Power Syst.*, 2011.
- [15] D. P. Bertsekas, *Nonlinear programming*, 2nd ed. Belmont (MA): Athena Scientific, 1999.
- [16] A. Ghosh, S. Boyd, and A. Saberi, "Minimizing effective resistance of a graph," *SIAM Rev.*, vol. 50, no. 1, pp. 37–66, Feb. 2008.
- [17] A. Gómez-Expósito, A. J. Conejo, and C. Cañizares, *Electric energy systems. Analysis and operation*. CRC Press, 2009.
- [18] S. Bolognani and S. Zampieri, "Convergence analysis of a distributed voltage support strategy for optimal reactive power compensation," in *Proc. NECSYS 2012, Santa Barbara (CA), USA*.
- [19] H. Uzawa, *Studies in linear and nonlinear programming*. Stanford University Press, 1958, ch. The Kuhn-Tucker theorem in concave programming, pp. 32–37.
- [20] D. P. Bertsekas and J. N. Tsitsiklis, *Parallel and Distributed Computation: Numerical Methods*. Athena Scientific, 1997.
- [21] R. D. Zimmerman, C. E. Murillo-Sánchez, and R. J. Thomas, "MATPOWER: steady-state operations, planning and analysis tools for power systems research and education," *IEEE Transactions on Power Systems*, vol. 26, no. 1, pp. 12–19, Feb. 2011.
- [22] L. Rogers and D. Williams, *Diffusions, Markov Processes and Martingales*, 2nd ed. Cambridge University Press, 1997.